# Shear modulus of neutron star crust

## D. A. Baiko\*

A. F. Ioffe Physical-Technical Institute, Politekhnicheskaya 26, 194021 St.-Petersburg, Russian Federation Saint-Petersburg State Polytechnical University, Politekhnicheskaya 29, 195251 St.-Petersburg, Russian Federation

Accepted; Received; in original form

#### ABSTRACT

Shear modulus of solid neutron star crust is calculated by thermodynamic perturbation theory taking into account ion motion. At given density the crust is modelled as a body-centered cubic Coulomb crystal of fully ionized atomic nuclei of one type with the uniform charge-compensating electron background. Classic and quantum regimes of ion motion are considered. The calculations in the classic temperature range agree well with previous Monte Carlo simulations. At these temperatures the shear modulus is given by the sum of a positive contribution due to the static lattice and a negative  $\propto T$  contribution due to the ion motion. The quantum calculations are performed for the first time. The main result is that at low temperatures the contribution to the shear modulus due to the ion motion saturates at a constant value, associated with zero-point ion vibrations. Such behavior is qualitatively similar to the zero-point ion motion contribution to the crystal energy. The quantum effects may be important for lighter elements at higher densities, where the ion plasma temperature is not entirely negligible compared to the typical Coulomb ion interaction energy. The results of numerical calculations are approximated by convenient fitting formulae. They should be used for precise neutron star oscillation modelling, a rapidly developing branch of stellar seismology.

**Key words:** dense matter – stars: neutron – white dwarfs – asteroseismology.

## I INTRODUCTION

Recent discovery of quasi-periodic oscillations (QPO) in soft gamma-repeaters (Israel et al. 2005; Strohmayer & Watts 2005; Watts & Strohmayer 2006) may be opening up an exciting possibility into studying neutron stars by methods of seismology. The QPO are thought to be related to neutron star vibrations and, in particular, originally, they were thought to be related to torsional vibrations of neutron star crust (Duncan 1998; Piro 2005).

Even though it is now understood that the mechanism of neutron star oscillations is likely more complex and involves global oscillations of crust and core, coupled by the frozen-in magnetic field (Levin 2006, 2007; Lee 2008), it is still possible that the actual oscillation frequencies are related to pure crustal frequencies, the important controlling factor being the magnetic field strength and geometry (Glampedakis, Samuelsson & Andersson 2006; Watts & Strohmayer 2007; van Hoven & Levin 2010, and references therein). The crustal torsional vibration frequencies are determined by the shear modulus of the solid neutron star crust. The main purpose of the present paper is to calculate this quantity.

\* E-mail:baiko@astro.ioffe.ru

The bulk of the neutron star crust is made of fully ionized ions (of varying charge Ze and mass M) in crystalline state, immersed in a nearly uniform strongly degenerate electron gas. More specifically, the ions form a crystal, if the local temperature T falls below the melting temperature  $T_{\rm m} = Z^2 e^2/(a\Gamma_{\rm m})$ , where  $\Gamma_{\rm m} \approx 175$ , and  $a = (4\pi n/3)^{-1/3}$  is the ion sphere radius (n is the ion number density,  $k_{\rm B} = 1$ ). Typically one assumes that the ion crystal is of body-centered cubic (bcc) type, as this structure is preferable thermodynamically for strictly uniform electron background.

The state of the electron subsystem depends on matter density. We shall limit ourselves to such (not too low) densities, where electrons are degenerate and ions are completely pressure ionized ( $\rho \gtrsim 10AZ$  g cm<sup>-3</sup>, where A is the ion mass number; see for discussion Pethick & Ravenhall 1995; Haensel, Potekhin & Yakovlev 2007). At these densities the model of uniform charge-compensating background of electrons is reasonably good. It gets progressively better with the growth of density becoming especially accurate at  $\rho \gg 10^6$  g cm<sup>-3</sup>, where electrons are ultrarelativistic. The crystal of fully ionized ions with the uniform background of electrons is known as the Coulomb crystal.

In inner crust, at densities above the neutron drip density  $\rho_{\rm d} \approx 4.3 \cdot 10^{11} \ {\rm g \ cm^{-3}}$ , in addition to the Coulomb

crystal of ions and electrons, there are neutrons not bound in the atomic nuclei. The details of neutron interactions with nuclei are not known very well. It seems plausible that the properties of a strictly static crystal, i.e. a crystal with nuclei fixed at their lattice nodes, are determined by Coulomb forces. By contrast, the motion of nuclei about the lattice nodes may be affected by the presence of neutrons. Lacking a good model of this effect, we shall assume that it can be described by an effective nucleus mass and renormalized ion plasma frequency within the framework of the Coulomb crystal model.

The main purpose of this paper is thus to study the shear modulus of the Coulomb crystal. The groundwork for this problem was laid down by Fuchs (1936), who calculated the shear modulus of the static bcc Coulomb lattice. More recently, Ogata & Ichimaru (1990) calculated the shear modulus of the bcc Coulomb crystal taking into account the motion of ions about their lattice nodes. In that work shear modulus was found numerically with the aid of Monte Carlo simulations (e.g., Brush et al. 1966). By the nature of the method, the motion of ions was treated classically. Strohmayer et al. (1991) further remarked that quantum effects were not important due to the smallness of the ion plasma temperature compared to the typical lattice electrostatic energy. Finally, Horowitz & Hughto (2008) calculated the shear modulus of the Coulomb crystal taking into account weak electron screening in the Thomas-Fermi model. This calculation was done numerically using molecular dynamics method. Again the motion of ions was strictly classic.

In this paper we shall use the thermodynamic perturbation theory to find the shear modulus of the Coulomb crystal with ion motion included in the harmonic lattice model framework. Unlike numerical methods of Ogata & Ichimaru (1990) and Horowitz & Hughto (2008) this approach is capable of tackling quantum effects. The quantum effects are known to be important especially for lighter elements at higher densities. Quantum effects in the problem of Coulomb crystal elastic moduli are studied for the first time.

In addition to the outermost envelope of the external crust, the Coulomb crystal model fails in the 'nuclear pasta' region of the inner crust at densities  $\rho \gtrsim 10^{14} \ \mathrm{g \ cm^{-3}}$ , where nuclei become nonspherical. Estimates of the shear modulus in this layer were reported by Pethick & Potekhin (1998).

Besides neutron star crusts, the Coulomb crystals are expected to form in solid cores of white dwarfs, to which the present results thus also apply.

#### 2 GENERAL THEORY

A Coulomb crystal is composed of ions with charge Ze, arranged in a crystal lattice with equilibrium lattice sites  $R_I$ , immersed in a rigid background of electrons (charge -e). Background volume element coordinates are denoted as r. Suppose the crystal is deformed uniformly. Then the lattice remains perfect, but its equilibrium nodes move to new locations  $X_I$ . The background volume element r shifts to a new position r. Using the displacement gradients r0 and r1 are r2 and r3 are constant on r3. In the coordinates of the new positions via those

of the old ones as

$$X_{\alpha} = R_{\alpha} + u_{\alpha\beta}R_{\beta} , \qquad (1)$$

$$x_{\alpha} = r_{\alpha} + u_{\alpha\beta}r_{\beta} . \tag{2}$$

In this case, greek indices denote Cartesian coordinates. We do not distinguish between upper and lower indices, and summation over repeated greek indices from 1 to 3 is always assumed. The potential energy U of a uniformly deformed Coulomb crystal can be written as

$$\frac{U}{Z^{2}e^{2}} = \frac{1}{2} \sum_{IJ}' \frac{1}{|\mathbf{X}_{I} + \mathbf{u}_{I} - \mathbf{X}_{J} - \mathbf{u}_{J}|} - \sum_{I} \int \frac{n \, d\mathbf{r}}{|\mathbf{X}_{I} + \mathbf{u}_{I} - \mathbf{x}|} + \frac{n^{2}}{2} \iint \frac{d\mathbf{r}_{1} d\mathbf{r}_{2}}{|\mathbf{x}_{1} - \mathbf{x}_{2}|}, \quad (3)$$

where  $u_I$  is the I-th ion deviation from its deformed equilibrium position  $X_I$  due to thermal and zero-point vibrations, and n is the ion number density in the nondeformed configuration  $\{R\}$ . Integrations are over the nondeformed crystal volume V, prime means that terms with I = J are omitted. Since a crystal lattice realizes a local energy minimum with respect to small ion deviations from the lattice nodes, the energy U can be approximately expressed as

$$U \approx U^{\rm st}(\{\boldsymbol{X}\}) + \delta U , \qquad (4)$$

where  $U^{\text{st}}(\{X\})$  is the potential energy of the static deformed lattice (i.e. the energy of the lattice with all ions located at the lattice nodes), and  $\delta U$  is the second order term of the Taylor expansion in powers of  $u_I$ :

$$\delta U = \frac{1}{2} \sum_{IJ} \frac{\partial^2 U}{\partial u_I^{\mu} \partial u_J^{\nu}} u_I^{\mu} u_J^{\nu} \equiv \frac{1}{2} \sum_{IJ} U_{IJ}^{\mu\nu} u_I^{\mu} u_J^{\nu} , \qquad (5)$$

$$\frac{U_{IJ}^{\mu\nu}}{Z^{2}e^{2}} = \frac{\partial^{2}}{\partial X_{I}^{\mu}\partial X_{I}^{\nu}} \left\{ \frac{\delta_{IJ} - 1}{|\mathbf{X}_{I} - \mathbf{X}_{J}|} + \sum_{K \neq I} \frac{\delta_{IJ}}{|\mathbf{X}_{I} - \mathbf{X}_{K}|} - \delta_{IJ} \int \frac{n \, \mathrm{d}\mathbf{r}}{|\mathbf{X}_{I} - \mathbf{x}|} \right\}.$$
(6)

The last term in the curly brackets serves to cancel an infinity arising in the second one.

The potential energy of the static deformed lattice can be expanded in powers of the displacement gradients as follows

$$\frac{1}{V}U^{\text{st}}(\{\boldsymbol{X}\}) = \frac{1}{V}U^{\text{st}}(\{\boldsymbol{R}\}) + S_{\alpha\beta}^{\text{st}}u_{\alpha\beta} + \frac{1}{2}S_{\alpha\beta\gamma\lambda}^{\text{st}}u_{\alpha\beta}u_{\gamma\lambda}.$$
(7)

In this case,  $U^{\rm st}(\{R\})$  is the potential energy of the static nondeformed lattice, while the first order expansion coefficient  $S^{\rm st}_{\alpha\beta}$  can be expressed via electrostatic crystal pressure:  $S^{\rm st}_{\alpha\beta} = -P^{\rm st}\delta_{\alpha\beta}$  [note, that to first order  $\delta V/V = u_{\alpha\alpha}$  for an arbitrary deformation, where  $\delta V$  is the volume change due to the deformation; also see Sect. 3 and Wallace (1967)].  $S^{\rm st}_{\alpha\beta\gamma\lambda}$  are the static lattice elastic coefficients. Elastic coefficients as second derivatives with respect to the displacement gradients were introduced by Huang (1950).

Since the static lattice coefficients are well known (Fuchs 1936, see also Sect. 6), the main subject of the present paper is the temperature and density dependences of the elastic coefficients associated with ion vibrations about their lattice sites. Thus we shall focus on  $\delta U$  of Eqs. (4) and (5). Making use of the standard in solid-state theory (e.g., Born & Huang 1954) collective coordinates  $A_k^{\mu}$  (for brevity

of notation we consider simple lattices only, i.e. lattices with only one ion in the elementary cell):

$$u_I^{\mu} = \frac{1}{\sqrt{MN}} \sum_{\mathbf{k}} A_{\mathbf{k}}^{\mu} \exp\left(\mathrm{i}\mathbf{k} \cdot \mathbf{R}_I\right) ,$$
 (8)

where wavevector k belongs to the first Brillouin zone of the nondeformed lattice, while M and N are the ion mass and total number,  $\delta U$  can be written as

$$\delta U = \frac{1}{2MN} \sum_{\mathbf{k}\mathbf{k}'} A_{\mathbf{k}}^{\mu} A_{\mathbf{k}'}^{\nu}$$

$$\times \sum_{IJ} U_{IJ}^{\mu\nu} \exp\left[i\mathbf{k} \cdot (\mathbf{R}_I - \mathbf{R}_J) + i(\mathbf{k} + \mathbf{k}') \cdot \mathbf{R}_J\right]. (9)$$

At fixed J, the sum over I in Eq. (9), along with the sum over K and the integral in Eq. (6), can be extended to infinity. The remaining finite sum over J in Eq. (9) produces  $N\delta_{-kk'}$ . Then  $\delta U$  can be rewritten as

$$\delta U = \frac{Z^{2}e^{2}}{2M} \sum_{\mathbf{k}} A_{\mathbf{k}}^{\mu} A_{-\mathbf{k}}^{\nu} \sum_{I \neq 0} [1 - \exp\left(i\mathbf{k} \cdot \mathbf{R}_{I}\right)] \frac{\partial^{2} X_{I}^{-1}}{\partial X_{I}^{\mu} \partial X_{I}^{\nu}}$$

$$\equiv \frac{1}{2} \sum_{\mathbf{k}} A_{\mathbf{k}}^{\mu} A_{-\mathbf{k}}^{\nu} D^{\mu\nu}(\mathbf{k}, \{\mathbf{X}\}) , \qquad (10)$$

where the deformed dynamic matrix  $D^{\mu\nu}(\boldsymbol{k},\{\boldsymbol{X}\})$  has been introduced. That matrix can also be expanded in powers of the displacement gradients and thus related to higher order nondeformed lattice energy derivatives:

$$D^{\mu\nu}(\mathbf{k}, \{\mathbf{X}\}) \approx D^{\mu\nu}(\mathbf{k}, \{\mathbf{R}\}) + D^{\mu\nu}_{\alpha\beta}(\mathbf{k}) u_{\alpha\beta}$$

$$+ \frac{1}{2} D^{\mu\nu}_{\alpha\beta\gamma\lambda}(\mathbf{k}) u_{\alpha\beta} u_{\gamma\lambda} , \qquad (11)$$

$$D^{\mu\nu}_{\alpha\beta}(\mathbf{k}) = \frac{Z^2 e^2}{M} \sum_{\mathbf{R}}' [1 - \exp{(i\mathbf{k} \cdot \mathbf{R})}] R_{\beta}$$

$$\times \frac{\partial^3 R^{-1}}{\partial R_{\alpha} \partial R_{\mu} \partial R_{\nu}} , \qquad (12)$$

$$D^{\mu\nu}_{\alpha\beta\gamma\lambda}(\mathbf{k}) = \frac{Z^2 e^2}{M} \sum_{\mathbf{R}}' [1 - \exp{(i\mathbf{k} \cdot \mathbf{R})}] R_{\beta} R_{\lambda}$$

$$\times \frac{\partial^4 R^{-1}}{\partial R_{\alpha} \partial R_{\nu} \partial R_{\nu} \partial R_{\nu}} . \qquad (13)$$

The prime means that summations over  $\mathbf{R}$  run over all non-deformed lattice vectors except  $\mathbf{R}=0$ . Practical expressions for the coefficients of the expansion (11) can be found in Appendix A. They were obtained using the standard Ewald technique (e.g., Born & Huang 1954). In Eqs. (10), (12), and (13) it is understood that the apparent divergences are canceled by the electron background term of Eq. (6). In practical formulae of Appendix A this is reflected by the absence of the  $\mathbf{q}=0$  term in sums over reciprocal lattice vectors.

Nondeformed dynamic matrix  $D^{\mu\nu}(\mathbf{k}, \{\mathbf{R}\})$  is given by the expression for  $D^{\mu\nu}(\mathbf{k}, \{\mathbf{X}\})$ , stemming from Eq. (10), with  $X_I$  replaced by  $R_I$ . This matrix determines frequencies  $\omega_{\mathbf{k}j}$  and polarization vectors  $\mathbf{e}_{\mathbf{k}j}$  of nondeformed crystal oscillations:  $D^{\mu\nu}(\mathbf{k}, \{\mathbf{R}\})e^{\nu}_{\mathbf{k}j} = \omega^2_{\mathbf{k}j}e^{\mu}_{\mathbf{k}j}$ , where j enumerates oscillation modes with given  $\mathbf{k}$  (j=1,2,3) for simple lattices).

Let us expand  $A_k$  over the basis of  $e_{kj}$ :  $A_k^{\mu} = \sum_{j=1}^{3} e_{kj}^{\mu} Q_{kj}$ . Then the oscillatory potential energy (10)

shall consist of three parts  $\delta U = H_0 + H_1 + H_2$ , where

$$H_0 = \frac{1}{2} \sum_{kj} \omega_{kj}^2 Q_{kj} Q_{-kj} \tag{14}$$

$$H_1 = u_{\alpha\beta} \sum_{\mathbf{k}jj'} \frac{1}{2} \Phi_{\alpha\beta}^{jj'}(\mathbf{k}) Q_{\mathbf{k}j} Q_{-\mathbf{k}j'}$$
(15)

$$H_2 = \frac{1}{2} u_{\alpha\beta} u_{\gamma\lambda} \sum_{kjj'} \frac{1}{2} \Phi^{jj'}_{\alpha\beta\gamma\lambda}(\mathbf{k}) Q_{kj} Q_{-kj'} , \qquad (16)$$

and, following Born & Huang (1954), we have introduced quantities

$$\Phi_{\alpha\beta}^{jj'}(\mathbf{k}) = e_{\mathbf{k}j}^{\mu} e_{-\mathbf{k}j'}^{\nu} D_{\alpha\beta}^{\mu\nu}(\mathbf{k}) , \qquad (17)$$

$$\Phi_{\alpha\beta\gamma\lambda}^{jj'}(\mathbf{k}) = e_{\mathbf{k}j}^{\mu} e_{-\mathbf{k}j'}^{\nu} D_{\alpha\beta\gamma\lambda}^{\mu\nu}(\mathbf{k}) . \tag{18}$$

In this case,  $H_0$  is the oscillatory potential energy of the non-deformed lattice, while  $H_1$  and  $H_2$  represent a perturbation of this quantity due to the deformation.

In quantum mechanics coordinates  $Q_{kj}$  become operators. It is convenient to switch to second quantization representation, where operators  $Q_{kj}$  are expressed via phonon creation and annihilation operators  $a_{kj}^{\dagger}$  and  $a_{kj}$ :

$$Q_{kj} = \sqrt{\frac{\hbar}{2\omega_{kj}}} (a_{kj} + a^{\dagger}_{-kj}) ,$$

$$Q_{-kj} = \sqrt{\frac{\hbar}{2\omega_{kj}}} (a_{-kj} + a^{\dagger}_{kj}) .$$
(19)

It is now possible to obtain expansion of the free energy in powers of the displacement gradients using the thermodynamic perturbation theory (e.g., Landau & Lifshitz 1980):

$$\delta F = \sum_{n} V_{nn} w_{n} + \sum_{n,m}' \frac{|V_{nm}|^{2} w_{n}}{E_{n}^{(0)} - E_{m}^{(0)}} + \frac{1}{2T} \left[ \left( \sum_{n} V_{nn} w_{n} \right)^{2} - \sum_{n} (V_{nn})^{2} w_{n} \right] + \dots$$
(20)

In this case,  $V = H_1 + H_2$  is the perturbation operator, indices n and m run over all possible unperturbed quantum states (which in second quantization means a sum over all possible phonon occupation numbers in all modes), and  $w_n = \exp\{(F_0 - E_n^{(0)})/T\}$  is the probability of the quantum state n,  $F_0$  and  $E_n^{(0)}$  being unperturbed free energy and quantum state energy. Terms with n = m in the second sum are excluded.

For simple lattices,  $\mathbf{e}_{-\mathbf{k}j} = \mathbf{e}_{\mathbf{k}j}$ , while all matrices D on the r. h. s. of Eq. (11), are real and symmetric with respect to their upper indices  $\mu$  and  $\nu$ . Consequently, Eq. (20) can be written as  $(\delta F)/V = S^{\rm ph}_{\alpha\beta}u_{\alpha\beta} + 0.5S^{\rm ph}_{\alpha\beta\gamma\lambda}u_{\alpha\beta}u_{\gamma\lambda} + \dots$ , with

$$S_{\alpha\beta}^{\text{ph}} = \frac{1}{2V} \sum_{\mathbf{k}j} \Phi_{\alpha\beta}^{jj} \frac{\hbar}{2\omega_{\mathbf{k}j}} (1 + 2\bar{n}_{\mathbf{k}j}) , \qquad (21)$$

$$S_{\alpha\beta\gamma\lambda}^{\text{ph}} = \frac{1}{2V} \sum_{\mathbf{k}j} \frac{\hbar}{2\omega_{\mathbf{k}j}} (1 + 2\bar{n}_{\mathbf{k}j})$$

$$\times \left[ \Phi_{\alpha\beta\gamma\lambda}^{jj} - \frac{\Phi_{\alpha\beta}^{jj} \Phi_{\gamma\lambda}^{jj}}{2\omega_{\mathbf{k}j}^{2}} + 2 \sum_{j'\neq j} \frac{\Phi_{\alpha\beta}^{jj'} \Phi_{\gamma\lambda}^{jj'}}{\omega_{\mathbf{k}j}^{2} - \omega_{\mathbf{k}j'}^{2}} \right]$$

$$- \frac{1}{2V} \sum_{\mathbf{k}j} \frac{\hbar^{2}}{T} (\bar{n}_{\mathbf{k}j} + 1) \bar{n}_{\mathbf{k}j} \frac{\Phi_{\alpha\beta}^{jj} \Phi_{\gamma\lambda}^{jj}}{2\omega_{\mathbf{k}j}^{2}} , \qquad (22)$$

where  $\bar{n}_{kj} = [\exp{(\hbar \omega_{kj}/T)} - 1]^{-1}$  is the average occupation number in a Bose system, and the argument k is implicit for all  $\Phi$ 's. Note a typo in eq. (41.38) of Born & Huang (1954), which differs from our expression (22) by the absence of a factor 2 in front of the  $\sum_{j'\neq j}$  in square brackets. The term with the double sum over j and j' in Eq. (22) can be also written as

$$\frac{1}{V} \sum_{\mathbf{k}j,j'>j} \Phi_{\alpha\beta}^{jj'} \Phi_{\gamma\lambda}^{jj'} \frac{q_{\mathbf{k}j}^2 - q_{\mathbf{k}j'}^2}{\omega_{\mathbf{k}j}^2 - \omega_{\mathbf{k}j'}^2} \quad \text{with} \quad q_{\mathbf{k}j}^2 \equiv \frac{\hbar}{2\omega_{\mathbf{k}j}} (1 + 2\bar{n}_{\mathbf{k}j}) \;,$$

which removes the singularity associated with degenerate phonon modes  $\omega_{kj} = \omega_{kj'}$ .

The expansion of  $\delta F$  in powers of displacement gradients is done at fixed temperature. Accordingly, the elastic coefficients of Eq. (22) are isothermal. Adiabatic elastic coefficients are defined via expansion of energy in powers of displacement gradients at fixed entropy (see Sect. 5).

Besides the Huang expansion in powers of the displacement gradients it is customary to expand thermodynamic potentials in powers of the Lagrangian strain parameters

$$\eta_{\alpha\beta} = \frac{1}{2} (u_{\alpha\beta} + u_{\beta\alpha} + u_{\lambda\alpha} u_{\lambda\beta}) . \tag{23}$$

In this way one obtains  $(\delta F)/V = C_{\alpha\beta}\eta_{\alpha\beta} + 0.5C_{\alpha\beta\gamma\lambda}\eta_{\alpha\beta}\eta_{\gamma\lambda} + \dots$  Since expansions in terms of  $u_{\alpha\beta}$  and  $\eta_{\alpha\beta}$  must coincide, one has (Wallace 1967)

$$C_{\alpha\beta} = S_{\alpha\beta} ,$$

$$C_{\alpha\beta\gamma\lambda} = S_{\alpha\beta\gamma\lambda} - \delta_{\alpha\gamma}S_{\beta\lambda} ,$$
(24)

with the same relationships holding for partial contributions (e.g., 'st', 'ph', etc). Coefficients C have complete Voigt symmetry, that is  $C_{\alpha\beta\gamma\lambda} = C_{\beta\alpha\gamma\lambda} = C_{\gamma\lambda\alpha\beta}$ . In general, this is not the case for the S-coefficients. In cubic symmetry there are only three nontrivial C-coefficients  $C_{1111}$ ,  $C_{1122}$ , and  $C_{1212}$ . In Voigt notation they are known as  $C_{11}$ ,  $C_{12}$ , and  $C_{44}$ , respectively.

The results of numerical calculations of elastic coefficients are presented in Sect. 6.

### 3 RELATION TO PHONON PRESSURE

As shown, e.g., by Wallace (1967), in the presence of an initial stress in the nondeformed configuration,  $-S_{\alpha\beta}$  (whether isothermal or adiabatic) is equal to this stress. In the case of a Coulomb crystal in neutron star crust such initial stress is produced by pressure. Consequently,  $S_{\alpha\beta} = -P\delta_{\alpha\beta}$ , and  $S_{\alpha\beta\gamma\lambda} = -P\delta_{\alpha\gamma}\delta_{\beta\lambda} + C_{\alpha\beta\gamma\lambda}$ . It is thus clear that while  $C_{1212} = C_{1221}$ ,  $S_{1212} \neq S_{1221} = S_{1212} + P$ .

If the total free energy is a sum of several partial contributions, their first derivatives yield partial pressures. Just like  $S_{\alpha\beta}^{\rm st}$  in Eq. (7) is related to electrostatic crystal pressure,  $S_{\alpha\beta}^{\rm ph} = -P^{\rm ph}\delta_{\alpha\beta}$ , where  $P^{\rm ph}$  is the phonon pressure. Phonon pressure is found as a volume derivative of the phonon thermodynamic potential  $\Omega^{\rm ph}$ :

$$P^{\rm ph} = -\left(\frac{\partial\Omega^{\rm ph}}{\partial V}\right)_{\mu,T}, \qquad (25)$$

$$\Omega^{\text{ph}} = \sum_{\mathbf{k}j} \left\{ \frac{\hbar \omega_{\mathbf{k}j}}{2} + T \ln \left[ 1 - \exp \left( -\frac{\hbar \omega_{\mathbf{k}j}}{T} \right) \right] \right\} .$$
(26)

The first and second terms in Eq. (26) describe zero-point

and thermal motion, respectively. The volume dependence is contained only in phonon frequencies. The ratios of phonon frequencies to the ion plasma frequency  $\omega_{\rm p}=\sqrt{4\pi nZ^2e^2/M}$  are universal functions for a given lattice type, and thus  $\omega_{{\bf k}j}\propto\omega_{\rm p}\propto n^{1/2}\propto V^{-1/2}.$  It follows, that

$$P^{\text{ph}} = \frac{1}{2V} \sum_{\mathbf{k}j} \left\{ \frac{\hbar \omega_{\mathbf{k}j}}{2} + \frac{\hbar \omega_{\mathbf{k}j}}{\exp(\hbar \omega_{\mathbf{k}j}/T) - 1} \right\}$$
$$= \frac{1}{4V} \sum_{\mathbf{k}j} \hbar \omega_{\mathbf{k}j} (1 + 2\bar{n}_{\mathbf{k}j}) . \tag{27}$$

We can, therefore, assert the following identity:

$$\sum_{\mathbf{k}j} \left( \frac{\Phi_{\alpha\beta}^{jj}}{\omega_{\mathbf{k}j}} + \omega_{\mathbf{k}j} \delta_{\alpha\beta} \right) (1 + 2\bar{n}_{\mathbf{k}j}) = 0 . \tag{28}$$

This identity can be proven directly (at least for bcc lattice). First, we notice that from Eq. (17) together with explicit formulae (A1) and (A2) from Appendix A, it is clear that  $\Phi_{xy}^{jj}(\mathbf{k}_1) = -\Phi_{xy}^{jj}(\mathbf{k}_2)$ , where  $\mathbf{k}_1$  and  $\mathbf{k}_2$  differ from each other by the sign of their x-coordinate (or y-coordinate) and likewise for  $\Phi_{\alpha\beta}^{jj}$  with other pairs of indices  $\alpha \neq \beta$ . By contrast,  $\Phi_{xx}^{jj}$ ,  $\Phi_{yy}^{jj}$ , and  $\Phi_{zz}^{jj}$  do not change under a sign change of any of their argument coordinates. If, on the other hand,  $k_1$  and  $\mathbf{k}_2$  differ by the interchange of x- and y-coordinates, then  $\Phi_{xx}^{jj}(\mathbf{k}_1) = \Phi_{yy}^{jj}(\mathbf{k}_2), \ \Phi_{zz}^{jj}(\mathbf{k}_1) = \Phi_{zz}^{jj}(\mathbf{k}_2),$  and likewise for interchange of x- and z- or y- and z-coordinates. This means that  $\sum_{i=1}^{48} \Phi_{\alpha\beta}^{jj}(\mathbf{k}_i) = 16 [\Phi_{xx}^{jj}(\mathbf{k}) + \Phi_{yy}^{jj}(\mathbf{k}) + \Phi_{zz}^{jj}(\mathbf{k})] \delta_{\alpha\beta}$ . The sum on the l. h. s. is over 48 Brillouin zone vectors (with identical length  $|\mathbf{k}|$ ), obtained from  $\mathbf{k}$  by 6 possible permutations of absolute values of its Cartesian coordinates and, for each permutation, by 8 possible combinations of signs assigned to those coordinates.

For uniform compression  $\delta\omega_{kj} = -\omega_{kj}\delta V/(2V)$  and  $u_{\alpha\beta} = \delta_{\alpha\beta}\delta V/(3V)$ . On the other hand,  $\omega_{kj}^2 = e_{kj}^{\mu}e_{-kj}^{\nu}D^{\mu\nu}(k,\{R\})$ , and therefore,  $\delta\omega_{kj}^2 = u_{\alpha\beta}\Phi_{\alpha\beta}^{jj}$ , because variation of a polarization vector must be orthogonal to it in order to maintain its unit length. Combining these results we obtain  $\Phi_{\gamma\gamma}^{jj} = -3\omega_{kj}^2$ , which proves Eq. (28). It is obvious from the derivation, that in place of  $(1 + 2\bar{n}_{kj})$  we can have an arbitrary function of |k| and j.

#### 4 EFFECTIVE SHEAR MODULUS

Free energy expansion coefficients, introduced in Sect. 2, also determine elastic stress tensor of deformed crystal. If deformation with displacement gradient  $u_{\alpha\beta}$  is applied to a configuration under initial isotropic pressure P, the stress tensor  $\sigma_{\alpha\beta}$ , equal initially to  $-P\delta_{\alpha\beta}$ , will change by (Wallace 1967)

$$\delta\sigma_{\alpha\beta} = \frac{1}{2}B_{\alpha\beta\gamma\lambda}(u_{\gamma\lambda} + u_{\lambda\gamma}) , \qquad (29)$$

where

$$B_{\alpha\beta\gamma\lambda} = S_{\alpha\beta\gamma\lambda} - P(\delta_{\alpha\lambda}\delta_{\beta\gamma} - \delta_{\alpha\beta}\delta_{\gamma\lambda}) \ . \tag{30}$$

Thus 
$$B_{1111} = S_{1111}$$
,  $B_{1122} = S_{1122} + P$ ,  $B_{1212} = S_{1212} = B_{1221}$ .

Expression (29) allows one to write down linearized elastic medium equation of motion. In nonuniform matter  $\delta\sigma_{\alpha\beta}$  of Eq. (29) gives Lagrangian variation of the stress tensor. In realistic neutron star modelling, equation of motion must also take into account magnetic field and non-uniformity of

matter and initial stress, associated with gravitation [cf., e.g., eq. (9) in Carroll et al. (1986)]. If all these complications are omitted, the equation of motion reads [eq. (2.23) of Wallace (1967)]

$$\rho \ddot{u}_{\alpha} = B_{\alpha\beta\gamma\lambda} \frac{\partial^{2} u_{\gamma}}{\partial R_{\beta} \partial R_{\lambda}} = S_{\alpha\beta\gamma\lambda} \frac{\partial^{2} u_{\gamma}}{\partial R_{\beta} \partial R_{\lambda}} , \qquad (31)$$

where  $\rho$  is the nondeformed mass density and  $\boldsymbol{u}$  is the displacement (so that  $\boldsymbol{X} = \boldsymbol{R} + \boldsymbol{u}$ ).

In Fourier space one has

$$\rho \omega^2 u^2 = S_{\alpha\beta\gamma\lambda} u_{\alpha} u_{\gamma} k_{\beta} k_{\lambda} , \qquad (32)$$

which for cubic symmetry can be expanded as

$$\rho\omega^{2}u^{2} = S_{1111}(u_{x}^{2}k_{x}^{2} + u_{y}^{2}k_{y}^{2} + u_{z}^{2}k_{z}^{2})$$

$$+ 2S_{1122}(u_{x}k_{x}u_{y}k_{y} + u_{x}k_{x}u_{z}k_{z} + u_{z}k_{z}u_{y}k_{y})$$

$$+ 2S_{1221}(u_{x}k_{x}u_{y}k_{y} + u_{x}k_{x}u_{z}k_{z} + u_{z}k_{z}u_{y}k_{y})$$

$$+ S_{1212}(u_{x}^{2}k_{y}^{2} + u_{y}^{2}k_{z}^{2} + u_{x}^{2}k_{z}^{2}$$

$$+ u_{z}^{2}k_{x}^{2} + u_{y}^{2}k_{z}^{2} + u_{z}^{2}k_{y}^{2}).$$

$$(33)$$

From Eqs. (29) and (33) it is clear that in a perfect crystal it is  $B_{1212} = S_{1212}$  that produces a response to a shear deformation. For this reason we shall call  $S_{1212}$  the elastic shear coefficient. However, it was proposed by Ogata & Ichimaru (1990) that in order to describe transverse modes in neutron star crusts, presumably composed of many small randomly oriented crystalline domains, one has to consider a directional average of the above equation. In particular, one has to average over directions of  $\boldsymbol{u}$  perpendicular to  $\boldsymbol{k}$  and then over all possible directions of  $\boldsymbol{k}$ . The resulting isotropic phase velocity  $\omega/k$  should then be equated to effective shear wave speed  $\sqrt{\mu_{\rm eff}/\rho}$ , where  $\mu_{\rm eff}$  is the effective shear modulus. The Lagrangian stress tensor variation is then approximated by the isotropic medium expression [e.g., eq. (15) in Carroll et al. (1986)] with  $\mu_{\rm eff}$  in place of the shear modulus.

The necessary averaging is easy to carry out. Firstly,

$$\langle u_{\alpha}u_{\beta}\rangle = \frac{u^2}{2} \left(\delta_{\alpha\beta} - \frac{k_{\alpha}k_{\beta}}{k^2}\right).$$
 (34)

And secondly, averaging over angles of k yields

$$\frac{\rho\omega^2}{k^2} = \frac{1}{5}(S_{1111} - S_{1122} - S_{1221} + 4S_{1212}) \ . \tag{35}$$

The combination on the r. h. s. of Eq. (35) is just the effective shear modulus  $\mu_{\rm eff}$  in question.

It is not quite clear whether this averaging oversimplifies the real situation in neutron star crust. Firstly, it is not known how small and randomly oriented the crystalline domains making up the crust really are, and whether or not one should consider instead a more regular crystal structure. For instance, as shown by Baiko (2009), bcc Coulomb crystal in magnetic field has minimum energy, if it is oriented so that the direction of the magnetic field coincides with the direction towards one of the nearest neighbors. This effect is due to a dependence of zero-point energy on mutual orientation of the magnetic field and crystal axes. So, it is easy to imagine that during star cooling the crust solidifies in such a way that the direction towards a nearest neighbor coincides with that of the magnetic field. This will produce a large scale ordered crystal structure. Secondly, if we agree with the notion of crust as a collection of small randomly oriented domains, it is not Eq. (31) that has to be averaged, but the full equation of motion, which differs from (31) by the presence of important anisotropies due to magnetic field and gravitation.

Since  $\mu_{\rm eff}$  contains all elastic coefficients (e.g.,  $S_{1111}$  which is related to bulk compressibility) one may wonder whether any other subsystem, besides the ion lattice, contributes to  $\mu_{\rm eff}$ . If a partial contribution to the energy (or the free energy) is a function of particle density only (e.g. kinetic energy of the degenerate electron gas), the Huang coefficients, associated with it, can be written as

$$VS_{\alpha\beta\gamma\lambda} = \frac{\partial^{2}U}{\partial u_{\alpha\beta}\partial u_{\gamma\lambda}} = \frac{\partial^{2}n_{x}}{\partial u_{\alpha\beta}\partial u_{\gamma\lambda}} \frac{\partial U}{\partial n_{x}} + \frac{\partial n_{x}}{\partial u_{\alpha\beta}} \frac{\partial n_{x}}{\partial u_{\gamma\lambda}} \frac{\partial^{2}U}{\partial n_{x}^{2}}.$$
 (36)

In this case,  $n_x$  is the density in the deformed configuration which, to second order in displacement gradients, reads

$$n_{x} = \frac{n}{\det(1 + u_{\alpha\beta})} \approx n \left[ 1 - \text{Tr}(u_{\alpha\beta}) + u_{11}^{2} + u_{22}^{2} + u_{33}^{2} + u_{11}u_{22} + u_{11}u_{33} + u_{22}u_{33} + u_{13}u_{31} + u_{12}u_{21} + u_{23}u_{32} \right],$$
(37)

where n is the nondeformed density. Consequently, one finds

$$VS_{1111} = 2n\frac{\partial U}{\partial n_{x}} + n^{2}\frac{\partial^{2}U}{\partial n_{x}^{2}},$$

$$VS_{1122} = n\frac{\partial U}{\partial n_{x}} + n^{2}\frac{\partial^{2}U}{\partial n_{x}^{2}},$$

$$VS_{1221} = n\frac{\partial U}{\partial n_{x}},$$

$$VS_{1212} = 0.$$
(38)

The important implication is that there are no partial contributions to neither  $S_{1212}$  nor  $\mu_{\rm eff}$  [see Eq. (35)] due to such partial contributions to the (free) energy. In particular, neither electrons nor dripped neutrons (in the standard model of neutron gas, e.g., Shapiro & Teukolsky 1983) in neutron star crust contribute to the effective shear modulus.

## 5 ISOTHERMAL AND ADIABATIC ELASTIC COEFFICIENTS

In the previous sections we have found formulae for isothermal Huang coefficients  $S_{\alpha\beta\gamma\lambda}^{\rm ph}$  and effective shear modulus  $\mu_{\rm eff}^{\rm ph}=(S_{1111}^{\rm ph}-S_{1122}^{\rm ph}-S_{1221}^{\rm ph}+4S_{1212}^{\rm ph})/5$ . Adiabatic Huang coefficients may be defined in the same way, the only difference being that the energy is expanded in powers of displacement gradients  $u_{\alpha\beta}$  (instead of the free energy). Adiabatic coefficients are likely much more appropriate for neutron star seismology. In this section we show that isothermal and adiabatic  $S_{1212}$  as well as  $\mu_{\rm eff}$  are actually the same. In order to prove this, we note that

$$\left(\frac{\partial E}{\partial u_{\alpha\beta}}\right)_{S} = \frac{\partial(E,S)}{\partial(u_{\alpha\beta},T)} \frac{\partial(u_{\alpha\beta},T)}{\partial(u_{\alpha\beta},S)} 
= \left(\frac{\partial E}{\partial u_{\alpha\beta}}\right)_{T} - \left(\frac{\partial E}{\partial T}\right)_{u_{\alpha\beta}} \left(\frac{\partial S}{\partial u_{\alpha\beta}}\right)_{T} \left(\frac{\partial S}{\partial T}\right)_{u_{\alpha\beta}}^{-1} 
= \left(\frac{\partial E}{\partial u_{\alpha\beta}}\right)_{T} + \left(\frac{\partial E}{\partial T}\right)_{u_{\alpha\beta}} \left(\frac{\partial T}{\partial u_{\alpha\beta}}\right)_{S} .$$
(39)

Substituting

$$\left(\frac{\partial E}{\partial T}\right)_{u_{\alpha\beta}} = \left(\frac{\partial E}{\partial S}\right)_{u_{\alpha\beta}} \left(\frac{\partial S}{\partial T}\right)_{u_{\alpha\beta}} \tag{40}$$

into Eq. (39) we see that

$$\begin{split} \left(\frac{\partial E}{\partial u_{\alpha\beta}}\right)_{S} + \left(\frac{\partial E}{\partial S}\right)_{u_{\alpha\beta}} \left(\frac{\partial S}{\partial u_{\alpha\beta}}\right)_{T} \\ &= \left(\frac{\partial E}{\partial u_{\alpha\beta}}\right)_{S} + T\left(\frac{\partial S}{\partial u_{\alpha\beta}}\right)_{T} = \left(\frac{\partial E}{\partial u_{\alpha\beta}}\right)_{T} , \quad (41) \end{split}$$

where  $T=(\partial E/\partial S)_{u_{\alpha\beta}}$  was used. (Keeping displacement gradients  $u_{\alpha\beta}$  fixed ensures that the volume and shape of the crystal does not change.) Since F=E-TS, Eq. (41) means that

$$\left(\frac{\partial E}{\partial u_{\alpha\beta}}\right)_S = \left(\frac{\partial F}{\partial u_{\alpha\beta}}\right)_T .$$
(42)

Therefore

$$\left(\frac{\partial^{2} E}{\partial u_{\alpha\beta} \partial u_{\gamma\lambda}}\right)_{S} = \left[\frac{\partial}{\partial u_{\alpha\beta}} \left(\frac{\partial F}{\partial u_{\gamma\lambda}}\right)_{T}\right]_{S} \\
= \left(\frac{\partial^{2} F}{\partial u_{\alpha\beta} \partial u_{\gamma\lambda}}\right)_{T} + \left[\frac{\partial}{\partial T} \left(\frac{\partial F}{\partial u_{\gamma\lambda}}\right)_{T}\right]_{u_{\alpha\beta}} \left(\frac{\partial T}{\partial u_{\alpha\beta}}\right)_{S} . (43)$$

Expressing derivative of T from Eqs. (39) and using (42) we obtain

$$\left(\frac{\partial^{2} E}{\partial u_{\alpha\beta} \partial u_{\gamma\lambda}}\right)_{S} = \left(\frac{\partial^{2} F}{\partial u_{\alpha\beta} \partial u_{\gamma\lambda}}\right)_{T} + T\left(\frac{\partial S}{\partial u_{\alpha\beta}}\right)_{T} \left(\frac{\partial S}{\partial u_{\gamma\lambda}}\right)_{T} \left(\frac{\partial E}{\partial T}\right)_{u_{\alpha\beta}}^{-1} .$$
(44)

Since  $S = -(\partial F/\partial T)_{u_{\alpha\beta}}$ , and  $(\partial F/\partial u_{\alpha\beta})_T \propto \delta_{\alpha\beta}$  [i.e. zero for  $\alpha \neq \beta$  and same for all  $\alpha = \beta$ ; cf. proof of Eq. (28)], we see that there is no difference between adiabatic and isothermal Huang coefficients  $S_{1212}$  as well as  $S_{1221}$ . Also, we see that the difference between adiabatic and isothermal coefficients  $S_{1111}$  is the same as that for coefficients  $S_{1122}$ . This ensures that adiabatic and isothermal  $\mu_{\rm eff}$  are the same.

#### 6 NUMERICAL RESULTS

In this section we present results of numerical calculations of the elastic coefficients for the bcc lattice. For such a lattice, one only needs to calculate four coefficients entering Eq. (35),  $S_{1111}$ ,  $S_{1122}$ ,  $S_{1221}$ , and  $S_{1212}$ . All the other coefficients with 2 pairs of identical indices are equal to these ones (e.g.,  $S_{1111} = S_{2222} = S_{3333}$ ,  $S_{1212} = S_{2121} = S_{1313} = \ldots$ ,  $S_{1221} = S_{2112} = S_{1331} = \ldots$ ), while the rest of the coefficients are zero. Alternatively, one can calculate  $S_{1111}$ ,  $S_{1122}$ ,  $S_{1212}$ , and pressure P. In what follows we shall focus on static lattice and phonon contributions. As discussed in Sect. 4, there are no other contributions to the shear modulus.

The static lattice elastic coefficients are well-studied in the literature. Practical expressions for the coefficients of the expansion (7) can be found in Appendix B. They are derived using standard Ewald technique and given here for completeness. The numerical results obtained using these expressions are given in Table 1. These values agree with the results of Fuchs (1936), who calculated lattice energy expansion coefficients for two types of elastic deformations,  $A = -P^{\text{st}} + S_{1111}^{\text{st}} - S_{1122}^{\text{st}}$  and  $2B = S_{1212}^{\text{st}}$ , for bcc and face-centered cubic lattices (see also Wallace 1967).

Computation of phonon coefficients (22) requires integration over the first Brillouin zone,  $\sum_{\mathbf{k}} = (2\pi)^{-3} V \int d\mathbf{k}$ . Methods of such integration have been developed elsewhere (Albers & Gubernatis 1981; Baiko 2000; Baiko et al. 2001). It is sufficient to integrate only over the primitive cell of the Brillouin zone, described, for bcc lattice, by inequalities  $k_x \geqslant k_y \geqslant k_z \geqslant 0$  and  $k_x + k_y \leqslant 2\pi/a_l$ , where  $a_l$  is the bcc lattice constant:  $na_l^3 = 2$ . The phonon frequencies are even functions of  $k_x$ ,  $k_y$ ,  $k_z$  and are invariant under an arbitrary permutation of  $k_x$ ,  $k_y$ ,  $k_z$ . In order to formulate symmetry properties of other quantities entering (22) we denote an arbitrary permutation of (x, y, z) as  $(\rho, \sigma, \tau)$ . If one interchanges  $k_{\sigma} \rightleftharpoons k_{\tau}$  then  $\Phi_{\rho\rho\rho\rho}^{jj}$ ,  $\Phi_{\sigma\sigma\tau\tau}^{jj}$  (equal to  $\Phi_{\tau\sigma\sigma\sigma}^{jj}$ ),  $\Phi_{\sigma\tau\tau\sigma}^{jj}$  (equal to  $\Phi_{\tau\sigma\sigma\tau}^{jj}$ ) remain the same, whereas  $\Phi_{\sigma\sigma\sigma\sigma}^{jj} \rightleftharpoons \Phi_{\tau\tau\tau\tau}^{jj}$ , ern symmetry properties of products  $\Phi_{\alpha\beta}^{jj'}\Phi_{\gamma\lambda}^{jj'}$ , viewed as 4-index  $(\alpha\beta\gamma\lambda)$  quantities. Additionally,  $\Phi_{\sigma\sigma\tau\tau}^{jj} = \Phi_{\sigma\sigma\tau\sigma}^{jj}$ , and  $\Phi_{\sigma\tau}^{jj} = \Phi_{\tau\sigma}^{jj}$ , so that  $\Phi_{\sigma\tau}^{jj} \Phi_{\sigma\tau}^{jj} = \Phi_{\tau\sigma}^{jj} \Phi_{\tau\sigma}^{jj} = \Phi_{\sigma\tau}^{jj} \Phi_{\tau\sigma}^{jj}$ . Both  $\Phi_{\alpha\beta\gamma\lambda}^{jj}$  and products  $\Phi_{\alpha\beta}^{jj'}\Phi_{\gamma\lambda}^{jj'}$  are even functions of

Let us give the recipe to calculate an arbitrary  $S^{\rm ph}$  coefficient from Eq. (22). In order to obtain, for instance,  $S^{\rm ph}_{1111}$  one has to integrate over the primitive cell of the Brillouin zone the integrand in Eq. (22) with  $\alpha\beta\gamma\lambda = xxxx$ , yyyy, and zzzz. Then add the three results together and multiply by 16 to account for the remaining two permutations for positive  $k_x$ ,  $k_y$ ,  $k_z$  and for 8 possible combinations of signs of  $k_x$ ,  $k_y$ ,  $k_z$ . The same recipe is applied in the case of  $S^{\rm ph}_{1122}$  and  $S^{\rm ph}_{1221}$ .

The situation with  $S^{\rm ph}_{1212}$  is more complex because, for instance,  $\Phi^{jj}_{xyxy} \neq \Phi^{jj}_{yxyx}$ . This requires integration over the primitive cell of the integrand of Eq. (22) with  $\alpha\beta\gamma\lambda = xyxy, yxyx, xzxz, zxzx, yzyz$ , and zyzy, addition of all 6 of them together and multiplication by 8.

We shall now describe the results of numerical calculations. In Fig. 1 we show  $-S_{1212}^{\rm ph}$  (upper dashed curve) and  $-\mu_{\text{eff}}^{\text{ph}}$  (lower dashed curve) in units of  $nT_{\text{p}}$  as functions of  $T/T_{\rm p}$ , where  $T_{\rm p}=\hbar\omega_{\rm p}$  is the ion plasma temperature. Quantities  $S_{1212}^{\rm ph}$  and  $\mu_{\rm eff}^{\rm ph}$  are negative. Thus they reduce the respective static lattice values (Table 1) and weaken lattice resistance to the shear strain. Dots show the same quantities with quantum effects explicitly excluded. In this case the elastic coefficients are always proportional to T. These results are obtained by setting  $\bar{n}_{\boldsymbol{k}j} = T/\hbar\omega_{\boldsymbol{k}j}$  and retaining only the highest order terms in T in Eq. (22). At higher temperatures the classic curves merge with the exact results, whereas at lower temperatures the quantum effects dominate. The exact curves do not decrease beyond certain values corresponding to ion zero-point motion. In this temperature regime the perturbation theory has clear advantage over Monte Carlo or molecular dynamics methods, in which the ion motion is treated classically.

**Table 1.** Static lattice elastic coefficients (bcc) in units of  $nZ^2e^2/(2a_l)$ , where  $a_l$  is the bcc lattice constant:  $na_l^3=2$ .

$S_{1111}^{ m st}$	$S^{ m st}_{1122}$	$S^{ m st}_{1212}$	$-P^{\mathrm{st}}$	A	$\mu_{ ext{eff}}^{ ext{st}}$
-1.4848079	-0.47067387	0.74240395	1.2130778	0.19894377	0.48523113

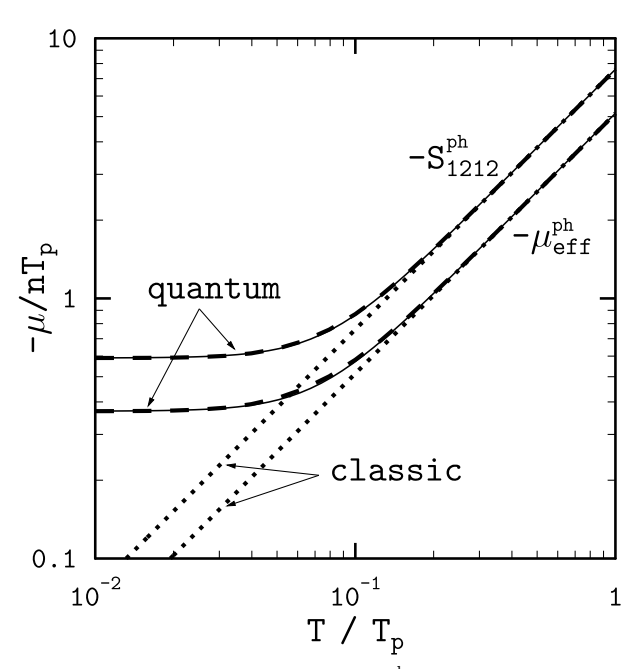


**Figure 1.** Phonon elastic coefficient  $-S_{1212}^{\rm ph}$  (upper dashed curve) and effective shear modulus  $-\mu_{\rm eff}^{\rm ph}$  (lower dashed curve) in units of  $nT_{\rm p}$  vs.  $T/T_{\rm p}$ . Solid curves and dots show analytic fits [Eqs. (45) and (46)] and classic numerical results, respectively.

We were able to fit the phonon shear coefficients as

$$\mu_{\text{eff}}^{\text{ph}} = -nT_{\text{p}} \left[ 0.3686^3 + 136.6 \left( \frac{T}{T_{\text{p}}} \right)^3 \right]^{1/3} ,$$
 (45)

$$S_{1212}^{\text{ph}} = -nT_{\text{p}} \left[ 0.5903^3 + 439 \left( \frac{T}{T_{\text{p}}} \right)^3 \right]^{1/3} .$$
 (46)

These curves are shown in Fig. 1 as thin solid lines (merging with the dashed ones). They reproduce exactly the classic and zero-point limits. The maximum error of the  $\mu_{\rm eff}^{\rm ph}$  fit is 2.2% at  $T/T_{\rm p} \approx 0.06$ . The maximum error of the  $S_{1212}^{\rm ph}$  fit is 1.0% at  $T/T_{\rm p} \approx 0.08$ .

If one subtracts the  $T\to 0$  limit (i.e. the zero-point contribution) from the phonon elastic coefficients, the remaining part will correspond to thermal ion motion (we denote this part by a superscript 'th'). In analogy with the derivation of the Debye  $T^3$ -law for specific heat, one can show that at low T this thermal contribution to the elastic coefficients behaves as  $T^4$  (e.g., Born & Huang 1954). In the classic regime of high T, both  $S^{\rm th}_{1212}$  and  $\mu^{\rm th}_{\rm eff}$  are, naturally, proportional to T (cf. Fig. 1). Our numerical calculations of  $-\mu^{\rm th}_{\rm eff}$  and  $-S^{\rm th}_{1212}$  reproduce both asymptotes and are shown in Fig. 2 by solid and dashed lines, respectively. Dots show the zero-point contribution to  $\mu^{\rm ph}_{\rm eff}$ . Since it is the sum of the zero-point and thermal contributions that make up the total phonon elastic coefficient, the  $T^4$  part of the thermal

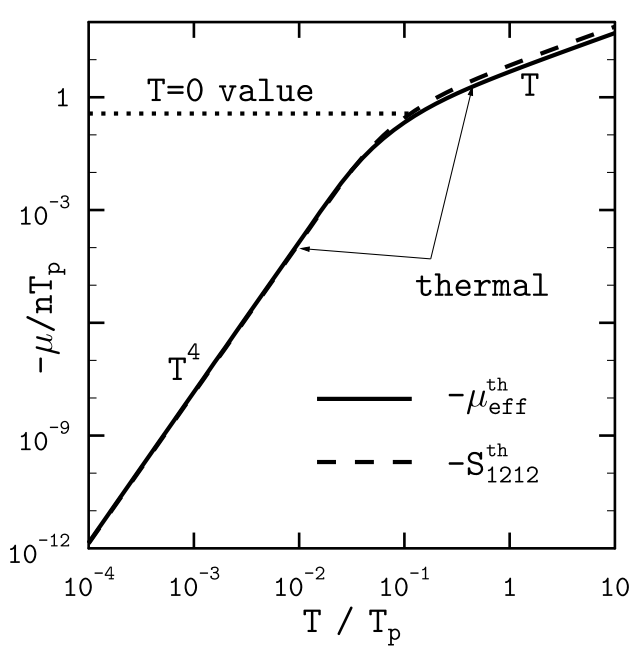


Figure 2. Thermal contributions  $-\mu_{\rm eff}^{\rm th}$  (solid line) and  $-S_{1212}^{\rm th}$  (dashed line) and zero-point contribution to  $-\mu_{\rm eff}^{\rm ph}$  (dots) in units of  $nT_{\rm p}$  vs.  $T/T_{\rm p}$ .

**Table 2.** Asymptote parameters f, g, and h in units of  $nT_{\rm p}$ , where  $f(T/T_{\rm p})^4$  is the thermal quantum asymptote,  $gT/T_{\rm p}$  is the classic asymptote, and h is the T=0 (zero-point) value of  $-\mu_{\rm eff}^{\rm ph}$  and  $-S_{121}^{\rm ph}$ .

	f	g	h
$-\mu_{ ext{eff}}^{ ext{ph}}$	$1.43 \times 10^{4}$	5.14	0.369
$-S_{1212}^{\mathrm{ph}}$	$1.35\times10^4$	7.60	0.590

contribution is practically always negligible. We summarize parameters of various asymptotes in Table 2.

Finally, let us compare our results with those of other authors. In Fig. 3 we show various approximations to the total effective shear modulus in units of  $nZ^2e^2/a$  versus  $\Gamma = Z^2e^2/(aT)$  for fully ionized  $^{12}\mathrm{C}$  at density  $10^{10}~\mathrm{g~cm^{-3}}$ . In this case  $a=(4\pi n/3)^{-1/3}$  is the ion-sphere radius and  $\Gamma$  is the standard Coulomb coupling parameter. Bars represent original Monte Carlo calculations of Ogata & Ichimaru (1990), while dash-dotted curve shows the fit to these data from Strohmayer et al. (1991). The solid line is  $\mu_{\mathrm{eff}}^{\mathrm{st}} + \mu_{\mathrm{eff}}^{\mathrm{ph}}$ , where  $\mu_{\mathrm{eff}}^{\mathrm{st}}$  is from Table 1 and  $\mu_{\mathrm{eff}}^{\mathrm{ph}}$  is given by Eq. (45). Dots show the sum of  $\mu_{\mathrm{eff}}^{\mathrm{st}}$  and the classic asymptote of  $\mu_{\mathrm{eff}}^{\mathrm{ph}}$  (dots in Fig. 1). This curve thus represents results of a purely classic calculation and may be directly compared with the Monte Carlo study. The dashed line shows results of molec-

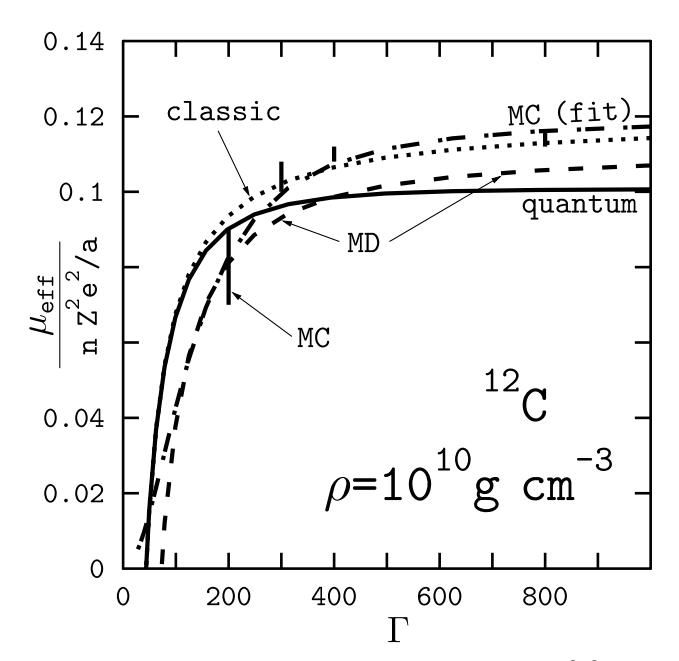


Figure 3. Total effective shear modulus in units of  $nZ^2e^2/a$  vs.  $\Gamma$  for fully ionized  $^{12}\mathrm{C}$  at density  $10^{10}$  g cm $^{-3}$ . Solid line and dots represent results of our quantum and classic calculations, respectively, bars show Monte Carlo (MC) data, dash-dotted curve is the fit to them, and dashed curve represents molecular dynamics (MD) results.

ular dynamics simulations reported by Horowitz & Hughto (2008).

First of all, we note that our classic calculation (dots) matches the bars of Ogata & Ichimaru (1990) with the exception of the one at  $\Gamma=200$ , where there is a discrepancy of about 3% between the dotted curve and the upper tip of the error bar. One possible reason for this discrepancy is associated with anharmonic corrections to the free energy, not taken into account in our perturbative calculation. At  $\Gamma=200$  the ratio of anharmonic and harmonic energies of the classic crystal is  $(A_1NT/\Gamma)/(3NT)\approx 1.8\%$ , where  $A_1\approx 10.84$  (Dubin 1990). On the other hand, it is not clear from Ogata & Ichimaru (1990) what is the confidence level of their error bars.

The difference between the quantum calculations (solid curve) and the classic ones depends on temperature and reflects the results shown in Fig. 1. The deviation of the quantum curve is mostly due to zero-point ion vibrations and is the strongest at lower temperatures (higher  $\Gamma$ 's). The relative magnitude of the deviation is proportional to  $a\hbar\omega_p/(Z^2e^2)\approx 0.05\rho_{10}^{1/6}/(Z_6A_{12}^{2/3}),$  where  $Z_6=Z/6,$   $A_{12}=A/12,$  and  $\rho_{10}$  is the mass density in units of  $10^{10}$  g cm $^{-3}$ . For carbon at  $\rho=10^{10}$  g cm $^{-3}$  and low T's, the classic effective shear modulus exceeds the more accurate quantum result by up to 18%.

As expected, at higher temperatures the quantum curve merges with the classic one. It is well known that for a Coulomb system the liquid state is energetically preferable to the crystal at  $\Gamma\lesssim 175$ . If there is a crystal at these  $\Gamma$ 's, it is in the metastable overheated state. We have extended our calculations into this temperature range for the sake of a qualitative discussion. Obviously, the further we go into the overheated crystal regime, the less accurate our re-

sults become due to the growing importance of anharmonic effects. In accordance with the general picture of Fig. 1, where the phonon contribution into the effective shear modulus is negative and grows by absolute value with temperature, the total effective shear modulus drops and, eventually, reaches zero at  $\Gamma \sim 45$ . This point should be regarded as a lower bound for the disappearance of the shear modulus in a Coulomb system. The actual crossing point is expected to occur at higher  $\Gamma$ 's and will be sensitive to the anharmonic effects

Molecular dynamics calculations of the effective shear modulus in a Coulomb system with compressible electron background, producing screening, were performed by Horowitz & Hughto (2008). These results are shown in Fig. 3 by the dashed line. The electron screening was described by the Thomas-Fermi (TF) model. By its nature the molecular dynamics approach does not take into account quantum effects. We observe a decrease of the shear modulus (with respect to the classic dotted curve) reflecting the fact that the crystal with screened Coulomb potential is less tightly bound than the pure Coulomb crystal.

It is well known that to lowest order in electromagnetic coupling, the screening by relativistic degenerate electrons is described by the (RPA) dielectric function of Jancovici (1962). The resulting effective ion-ion potential is more complex than the simple Yukawa potential arising in the TF model. Electron screening affects both properties of the static lattice and the phonon modes. As shown by Baiko (2002), the TF model overestimates the correction to the lattice electrostatic energy as compared to the more accurate RPA model. By contrast, the properties of the phonon modes obtained in the TF and RPA models are very similar. Since the main contribution to the effective shear modulus comes from the electrostatic energy, we expect, that calculations of Horowitz & Hughto (2008) in the TF model overestimate the importance of the electron background compressibility. It would be interesting (and is not difficult) to calculate the electrostatic contribution to the effective shear modulus using the full RPA model.

## 7 CONCLUSIONS

We have calculated elastic shear coefficient  $S_{1212}$  and effective direction averaged shear modulus  $\mu_{\rm eff}$  for neutron star crust matter. Both coefficients are sums of a static lattice term and a term originating from the motion of ions about their lattice nodes. While the static lattice contributions (Table 1) were well known previously, only numerical simulations existed for the ion motion terms. Using thermodynamic perturbation theory, we have expressed the ion motion terms via integrals over the first Brillouin zone of quantities given by rapidly convergent lattice sums, Eq. (22). The integrals were then evaluated numerically and the results were fitted by simple analytic formulae, Eqs. (45) and (46).

The main advantage of the numerical methods (Monte Carlo and molecular dynamics) is their ability to include anharmonic effects to all orders. The main advantage of the perturbation theory is its ability to include quantum effects (within the framework of the harmonic lattice model), greater transparency of the results and much lesser computer

time requirements. The anharmonic effects can also be taken into account in the perturbative approach, but that would make all the equations much more cumbersome even if only the lowest order anharmonic term is retained. Summarizing, we can say that numerical simulations and perturbation theory ideally complement each other as well as serve for mutual verification.

If quantum effects are included, one finds that the ion motion contribution can be decomposed into two parts. One of them corresponds to zero-point ion motion and is independent of T. The other corresponds to thermal ion motion and is  $\propto T^4$  at low temperatures and  $\propto T$  at high temperatures. The high T asymptote is what one obtains, if the calculation is purely classic. At low temperatures the thermal term is negligible compared to the zero-point term, and thus the  $T^4$  asymptote seems rather unimportant. Our fitting formulae (45) and (46) reproduce exactly the high T and zero-point limits.

If quantum effects are excluded, our results agree well (cf. dots and bars in Fig. 3) with Monte Carlo simulations of Ogata & Ichimaru (1990). The only discrepancy of about 3% occurs at  $\Gamma=200$ , where anharmonic effects are at their strongest (and also the error bars of the Monte Carlo simulation are at their largest). If quantum effects are included, then the main difference with the Monte Carlo results is due to the zero-point contribution to the ion motion term. Compared to the total shear modulus, that also includes the static lattice part, this contribution is important for lighter elements at higher densities, where the ion plasma temperature is not entirely negligible with respect to the typical Coulomb ion interaction energy.

We have demonstrated that neither  $S_{1212}$  nor  $\mu_{\rm eff}$  have any contributions from subsystems whose partial free energies are functions of particle number density only; that both coefficients are the same whether they are evaluated at constant temperature or entropy; we have also proven an identity linking phonon pressure with a coefficient of dynamic matrix expansion in powers of displacement gradients, Eq. (28).

The results, reported in this paper, also apply to crystallized matter in white dwarf cores.

#### ACKNOWLEDGMENTS

The author is grateful to D. G. Yakovlev for suggesting the topic of this research and numerous fruitful discussions. The work was supported by Ministry of Education and Science of Russian Federation (contract No. 11.G34.31.0001 with SPb-SPU and leading scientist G. G. Pavlov), by RFBR (grant 11-02-00253-a) and by Rosnauka (grant NSh 3769.2010.2).

## REFERENCES

Albers R.C., Gubernatis J.E., 1981, Los Alamos Scientific Laboratory Report No. LA-8674-MS

Baiko D.A., 2000, PhD thesis, A.F. Ioffe Physical-Technical Institute

Baiko D.A., Potekhin A.Y., Yakovlev D.G., 2001, Phys. Rev. E, 64, 057402

Baiko D.A., 2002, Phys. Rev. E, 66, 056405

Baiko D.A., 2009, Phys. Rev. E, 80, 046405

Born M., Huang K., 1954, Dynamical Theory of Crystal Lattices. Izdatelstvo inostrannoi literatury, Moscow

Brush S.G., Sahlin H.L., Teller E., 1966, J. Chem. Phys., 45, 2102

Carroll B.W., Zweibel E.G., Hansen C.J., McDermott P.N., Savedoff M.P., Thomas J.H., van Horn H.M., 1986, ApJ, 305, 767

Dubin D.H.E., 1990, Phys. Rev. A, 42, 4972

Duncan R.C., 1998, ApJ, 498, L45

Fuchs K., 1936, Proc. Roy. Soc. London, 153, 622

Glampedakis K., Samuelsson L., Andersson N., 2006, MN-RAS, 371, L74

Haensel P., Potekhin A.Y., Yakovlev D.G., 2007, Neutron Stars 1: Equation of State and Structure. Springer, New York

Horowitz C.J., Hughto J., 2008, preprint (astro-ph/0812.2650)

Huang K., 1950, Proc. Roy. Soc. A (London), 203, 178

Israel G.L. et al., 2005, ApJ, 628, L53

Jancovici B., 1962, Nuovo Cimento, 25, 428

Landau L.D., Lifshitz E.M., 1980, Statistical Physics. Part I. Pergamon Press, Oxford, eq. (32,5)

Lee U., 2008, MNRAS, 385, 2069

Levin Yu., 2006, MNRAS, 368, L35

Levin Yu., 2007, MNRAS, 377, 159

Ogata S., Ichimaru S., 1990, Phys. Rev. A, 42, 4867

Pethick C.J., Potekhin A.Y., 1998, Phys. Lett. B, 427, 7 Pethick C.J., Ravenhall D.G., 1995, Annu. Rev. Nucl. Part.

Piro A.L., 2005, ApJ, 634, L153

Sci., 45, 429

Shapiro S.L., Teukolsky S.A., 1983, Black Holes, White Dwarfs and Neutron Stars: The Physics of Compact Objects. Wiley-Interscience

Strohmayer T.E., Ogata S., Iyetomi H., Ichimaru S., van Horn H.M., 1991, ApJ, 375, 679

Strohmayer T.E., Watts A.L., 2005, ApJ, 632, L111

van Hoven M., Levin Yu., 2010, preprint (astro-ph/1006.0348)

Wallace D.C., 1967, Phys. Rev., 162, 776

Watts A.L., Strohmayer T.E., 2006, ApJ, 637, L117

Watts A.L., Strohmayer T.E., 2007, Adv. Sp. Res., 40, 1446

#### APPENDIX A:

Both  $D^{\mu\nu}_{\alpha\beta}({\pmb k})$  and  $D^{\mu\nu}_{\alpha\beta\gamma\lambda}({\pmb k})$  are sums of two series, over direct and reciprocal lattice vectors (denoted  ${\pmb R}$  and  ${\pmb G}$  respectively.

tively): 
$$D_{\alpha\beta}^{\mu\nu} = D_{\alpha\beta}^{\mu\nu[R]} + D_{\alpha\beta}^{\mu\nu[G]}, D_{\alpha\beta\gamma\lambda}^{\mu\nu} = D_{\alpha\beta\gamma\lambda}^{\mu\nu[R]} + D_{\alpha\beta\gamma\lambda}^{\mu\nu[G]}.$$

$$D_{\alpha\beta}^{\mu\nu[R]}(\mathbf{k}) = \frac{Z^2 e^2}{M} \sum_{\mathbf{R}}' [1 - \exp{(i\mathbf{k} \cdot \mathbf{R})}]$$

$$\times \left\{ \frac{4}{R^5} \left( \delta_{\alpha\mu} R_{\beta} R_{\nu} + \delta_{\alpha\nu} R_{\beta} R_{\mu} + \delta_{\mu\nu} R_{\alpha} R_{\beta} \right) \right.$$

$$\times \left[ \left( A^3 R^3 + \frac{3}{2} A R \right) \frac{e^{-A^2 R^2}}{\sqrt{\pi}} + \frac{3}{4} \operatorname{erfc}(AR) \right]$$

$$- \frac{8R_{\alpha} R_{\beta} R_{\mu} R_{\nu}}{R^7}$$

$$\times \left[ \left( A^5 R^5 + \frac{5}{2} A^3 R^3 + \frac{15}{4} A R \right) \frac{e^{-A^2 R^2}}{\sqrt{\pi}} + \frac{15}{8} \operatorname{erfc}(AR) \right] \right\}, \tag{A1}$$

$$D_{\alpha\beta}^{\mu\nu[G]}(\mathbf{k}) = \frac{4\pi n Z^{2} e^{2}}{M} \int \frac{\mathrm{d}\mathbf{q}}{q^{2}} \left[ \sum_{\mathbf{G}} \delta(\mathbf{q} - \mathbf{G}) - \sum_{\mathbf{G}} \delta(\mathbf{q} - \mathbf{k} - \mathbf{G}) \right] e^{-q^{2}/(4A^{2})} \times \left[ \delta_{\alpha\beta} q_{\mu} q_{\nu} + \delta_{\mu\beta} q_{\alpha} q_{\nu} + \delta_{\nu\beta} q_{\alpha} q_{\mu} - \frac{2}{q^{2}} \left( 1 + \frac{q^{2}}{4A^{2}} \right) q_{\alpha} q_{\beta} q_{\mu} q_{\nu} \right], \tag{A2}$$

$$D_{\alpha\beta\gamma\lambda}^{\mu\nu[R]}(\mathbf{k}) = \frac{Z^2 e^2}{M} \sum_{\mathbf{R}}' [1 - \exp\left(\mathrm{i}\mathbf{k} \cdot \mathbf{R}\right)]$$

$$\times \left\{ \frac{4R_{\beta}R_{\lambda}}{R^5} \left(\delta_{\alpha\gamma}\delta_{\mu\nu} + \delta_{\alpha\mu}\delta_{\gamma\nu} + \delta_{\alpha\nu}\delta_{\gamma\mu}\right) \right.$$

$$\times \left[ \left(A^3R^3 + \frac{3}{2}AR\right) \frac{e^{-A^2R^2}}{\sqrt{\pi}} + \frac{3}{4}\operatorname{erfc}(AR) \right]$$

$$- \frac{8R_{\beta}R_{\lambda}}{R^7} \left(\delta_{\alpha\gamma}R_{\mu}R_{\nu} + \delta_{\alpha\mu}R_{\gamma}R_{\nu} + \delta_{\alpha\nu}R_{\gamma}R_{\mu}\right.$$

$$+ \delta_{\gamma\mu}R_{\alpha}R_{\nu} + \delta_{\gamma\nu}R_{\alpha}R_{\mu} + \delta_{\mu\nu}R_{\alpha}R_{\gamma}\right)$$

$$\times \left[ \left(A^5R^5 + \frac{5}{2}A^3R^3 + \frac{15}{4}AR\right) \frac{e^{-A^2R^2}}{\sqrt{\pi}} \right.$$

$$+ \frac{15}{8}\operatorname{erfc}(AR) \right]$$

$$+ \frac{16R_{\alpha}R_{\beta}R_{\gamma}R_{\lambda}R_{\mu}R_{\nu}}{R^9}$$

$$\times \left[ \left(A^7R^7 + \frac{7}{2}A^5R^5 + \frac{35}{4}A^3R^3 + \frac{105}{8}AR\right) \right.$$

$$\times \frac{e^{-A^2R^2}}{\sqrt{\pi}} + \frac{105}{16}\operatorname{erfc}(AR) \right] \right\}, \quad (A3)$$

$$D_{\alpha\beta\gamma\lambda}^{\mu\nu[G]}(\mathbf{k}) = -\frac{4\pi n Z^{2} e^{2}}{M} \int \frac{d\mathbf{q}}{q^{2}} \left[ \sum_{\mathbf{G}}' \delta(\mathbf{q} - \mathbf{G}) - \sum_{\mathbf{G}} \delta(\mathbf{q} - \mathbf{k} - \mathbf{G}) \right] e^{-q^{2}/(4A^{2})} \times \left[ \delta^{(2)} q^{(2)} - \frac{2}{q^{2}} \left( 1 + \frac{q^{2}}{4A^{2}} \right) \delta q^{(4)} + \frac{8}{q^{4}} \left( 1 + \frac{q^{2}}{4A^{2}} + \frac{q^{4}}{32A^{4}} \right) q^{(6)} \right], \tag{A4}$$

where

$$\delta^{(2)}q^{(2)} = \delta_{\alpha\lambda} \left( \delta_{\gamma\beta}q_{\mu}q_{\nu} + \delta_{\mu\beta}q_{\gamma}q_{\nu} + \delta_{\nu\beta}q_{\gamma}q_{\mu} \right) 
+ \delta_{\gamma\lambda} \left( \delta_{\alpha\beta}q_{\mu}q_{\nu} + \delta_{\mu\beta}q_{\alpha}q_{\nu} + \delta_{\nu\beta}q_{\alpha}q_{\mu} \right) 
+ \delta_{\mu\lambda} \left( \delta_{\alpha\beta}q_{\gamma}q_{\nu} + \delta_{\gamma\beta}q_{\alpha}q_{\nu} + \delta_{\nu\beta}q_{\alpha}q_{\gamma} \right) 
+ \delta_{\nu\lambda} \left( \delta_{\alpha\beta}q_{\gamma}q_{\mu} + \delta_{\gamma\beta}q_{\alpha}q_{\mu} + \delta_{\mu\beta}q_{\alpha}q_{\gamma} \right) , \quad (A5)$$

$$\delta q^{(4)} = \delta_{\alpha\lambda}q_{\beta}q_{\gamma}q_{\mu}q_{\nu} + \delta_{\beta\lambda}q_{\alpha}q_{\gamma}q_{\mu}q_{\nu} + \delta_{\gamma\lambda}q_{\alpha}q_{\beta}q_{\mu}q_{\nu} 
+ \delta_{\mu\lambda}q_{\alpha}q_{\beta}q_{\gamma}q_{\nu} + \delta_{\nu\lambda}q_{\alpha}q_{\beta}q_{\gamma}q_{\mu} 
+ \delta_{\alpha\beta}q_{\gamma}q_{\mu}q_{\nu}q_{\lambda} + \delta_{\nu\beta}q_{\alpha}q_{\mu}q_{\nu}q_{\lambda} 
+ \delta_{\mu\beta}q_{\alpha}q_{\gamma}q_{\nu}q_{\lambda} + \delta_{\nu\beta}q_{\alpha}q_{\gamma}q_{\mu}q_{\lambda} , \quad (A6)$$

$$q^{(6)} = q_{\alpha}q_{\beta}q_{\gamma}q_{\lambda}q_{\mu}q_{\nu} . \quad (A7)$$

In the above equations, as well as in Appendix B, erfc is the complementary error function, and A is an arbitrary parameter with units of inverse length chosen so that sums over direct and reciprocal lattice vectors are equally rapidly convergent. Integrals over  $d\mathbf{q}$  in Eqs. (A2) and (A4) are kept for brevity of the formulae. They can be easily evaluated with the aid of the  $\delta$ -functions.

## APPENDIX B:

Similarly to Appendix A,  $S_{\alpha\beta}^{\rm st} = S_{\alpha\beta}^{[R]} + S_{\alpha\beta}^{[G]}$  and  $S_{\alpha\beta\gamma\lambda}^{\rm st} = S_{\alpha\beta\gamma\lambda}^{[R]} + S_{\alpha\beta\gamma\lambda}^{[G]}$ , where

$$S_{\alpha\beta}^{[R]} = -nZ^{2}e^{2}\sum_{\mathbf{R}}'\frac{R_{\alpha}R_{\beta}}{R^{3}}\left[\frac{AR}{\sqrt{\pi}}e^{-A^{2}R^{2}} + \frac{1}{2}\operatorname{erfc}(AR)\right] + \frac{n^{2}\pi Z^{2}e^{2}}{2A^{2}}\delta_{\alpha\beta},$$
(B1)

$$S_{\alpha\beta}^{[G]} = -2\pi n^2 Z^2 e^2 \sum_{G}' \frac{1}{G^2} \times \left[ \delta_{\alpha\beta} - \frac{2}{G^2} \left( 1 + \frac{G^2}{4A^2} \right) G_{\alpha} G_{\beta} \right] e^{-G^2/(4A^2)} , \text{ (B2)}$$

$$S_{\alpha\beta\gamma\lambda}^{[R]} = nZ^{2}e^{2}\sum_{R}' \left\{ \frac{2R_{\alpha}R_{\beta}R_{\gamma}R_{\lambda}}{R^{5}} \right.$$

$$\times \left. \left[ \left( A^{3}R^{3} + \frac{3}{2}AR \right) \frac{e^{-A^{2}R^{2}}}{\sqrt{\pi}} + \frac{3}{4}\operatorname{erfc}(AR) \right] \right.$$

$$- \delta_{\alpha\gamma}\frac{R_{\beta}R_{\lambda}}{R^{3}} \left[ \frac{AR}{\sqrt{\pi}}e^{-A^{2}R^{2}} + \frac{1}{2}\operatorname{erfc}(AR) \right] \right\}$$

$$- \frac{n^{2}\pi Z^{2}e^{2}}{2A^{2}} \left( \delta_{\alpha\beta}\delta_{\gamma\lambda} + \delta_{\alpha\lambda}\delta_{\beta\gamma} \right) , \tag{B3}$$

$$S_{\alpha\beta\gamma\lambda}^{[G]} = 2\pi n^2 Z^2 e^2 \sum_{G} \frac{1}{G^2} \left[ \left( \delta_{\alpha\beta} \delta_{\gamma\lambda} + \delta_{\alpha\lambda} \delta_{\beta\gamma} \right) \right]$$

$$- \frac{2}{G^2} \left( 1 + \frac{G^2}{4A^2} \right) \left( \delta_{\alpha\beta} G_{\gamma} G_{\lambda} + \delta_{\beta\gamma} G_{\alpha} G_{\lambda} \right)$$

$$+ \delta_{\beta\lambda} G_{\alpha} G_{\gamma} + \delta_{\alpha\lambda} G_{\beta} G_{\gamma} + \delta_{\gamma\lambda} G_{\alpha} G_{\beta} \right)$$

$$+ \frac{8}{G^4} \left( 1 + \frac{G^2}{4A^2} + \frac{G^4}{32A^4} \right) G_{\alpha} G_{\beta} G_{\gamma} G_{\lambda}$$

$$\times e^{-G^2/(4A^2)} . \tag{B4}$$